The Stretch Reflex Arc: Simulation, Control, and Identification*

A. Behal†, D.M. Dawson◇, P. Molnar‡, and J. Hickman‡

†Department of Electrical and Computer Engineering, Clarkson University, Potsdam, NY 13699

◇Department of Electrical and Computer Engineering, Clemson University, Clemson, SC 29634-0915

‡Nanoscience and Technology Center, University of Central Florida, Orlando, FL 32816

E-mail: abehal@clarkson.edu; ddawson@ces.clemson.edu; pmolnar,jhickman@mail.ucf.edu

Abstract

In this paper, we present simulation results for the closed-loop response of the reflex arc under variable stimuli and supraspinal commands. The data obtained can be utilized to quantify the control of movement imposed by the brain, *i.e.*, control signals mimicking the brain input can be derived such that a desired equilibrium muscle length or the tracking of a desired limb trajectory in time is possible. Simulation data obtained in this study will be utilized as a first order approximation of the supraspinal control effort. In order to test the validity of the simulation results, we also propose the construction of experimental testbeds for the identification of various sub-components of the reflex arc that have been developed in-vitro from cellular components.

1 Introduction

In nature, the muscle-reflex mechanism forms a feedback system called the motor servo [1, 2] consisting of a muscle, its spindle receptors, and the corresponding reflex pathways back to the muscle. This neuromuscular system mediates the stretch and unloading reflex of the muscle by feedback. To replicate the muscle-reflex system, Gielen [3] proposed a model of the motor servo that incorporated a nonlinear description of the behavior of muscle spindle receptors, a delay in the reflex loop via the spinal cord, and a nonlinear model describing muscle mechanical properties. Simulation studies and mathematical modular modeling of neural components were reported by He [4] by utilizing linear/nonlinear models from *in-vivo* experimental studies for the motoneuron, muscle dynamics, muscle mechanics, and spindle dynamics. Other researchers [5, 6, 7] have also reported various nonlinear muscle models. Utilizing the model of Hodgkin and Huxley, Ghosh [8] showed how analog signals could be

*This research was supported in part by National Multiple Sclerosis Society PP1069. A part of this paper was presented at the SAB 2002 *Workshop on Motor Control in Humans and Robots* in Edinburgh.

†Corresponding Author

represented by spike trains akin to those associated with a population of neurons. Concurrently, researchers have been fabricating elements of the reflex arc from cellular components. Previous work has shown that each element of the spinal reflex arc can be isolated, purified and grown *in-vitro* [9, 10, 11, 12, 13, 14]. Given extensive modeling data reported in literature culled from *in-vivo* experiment, identification of models for *in-vitro* elements can be initiated with the *in-vivo* models offering a first approximation. *In-vitro* identification and control of nonlinearities associated with the reflex arc is a challenging task; however, for over a decade, tremendous progress has been made in the field of nonlinear control systems. Modeling and control techniques have been developed for many types of systems with soft/hard nonlinearities (*e.g.*, mechanical systems with nonlinear friction effects [15, 16] and electrical systems with nonlinear saturation [17, 18] have been studied). Once the models for the *in-vitro* components are in place, it is postulated that nonlinear control techniques can be applied to derive analytical control algorithms that would proffer a better understanding of the modulation that the supraspinal control imposes on the neuromuscular system.

In this paper, models are detailed for the components of the reflex arc that are of analytical interest. These models, culled from extant literature, have mostly been identified via laboratory experiments *in-vivo*. In the Nanoscience Center at the University of Central Florida (UCF), components of the reflex arc are being manufactured from cellular components *in-vitro*. Since uniform conditions can be applied to a culture across a set of experiments to gather input-output data, the identified models from in-vitro experiments are expected to have more statistical significance. Thus, existing *in-vivo* models serve as a starting point for identification of *in-vitro* components. While identification experiments are being pursued concurrently, this research focused on obtaining a cohesive set of models for the various components of the reflex arc that (when integrated) would be able to reproduce the response of the stretch arc. The next step in the research involved a systems analysis of the simulated characteristics of the transient and steady-state response of the arc in order to be able to attribute those to one or more components in the loop. Furthermore, a map is envisaged between descending supraspinal inputs and muscle motion – this map is a precursor to identifying the supraspinal commands via mathematical constructs that do not hyperinflate in terms of computational intensity as the number of states increases. Finally, we also present a few experimental results concerning motoneuron electrophysiological characterization while we lay out the draft for construction of experimental testbeds, instrumentation, and procedures for identification of the remainder of the cultured elements of the reflex arc.

The rest of the paper is organized as follows. In Section 2, we discuss the models that we would adopt for the sub-components of the reflex arc (In this first study, the effect of Golgi Tendon Organs (GTO) have not been considered). Section 3 defines the mathematical problem that we are interested in looking at. In Section 4, we will present the results of the simulation studies as well as a discussion of the results obtained. In Section 5, we propose to build this simulation model to account for ascending information in the spinal cord and derive models that assimilate the aforementioned information and emanate descending command signals; nonlinear time-domain control strategies would result in better analytical models as opposed to existing models based on *ad-hoc* techniques. Preliminary results concerning experimental implementation and testing of the stretch reflex arc *in-vitro* are presented in Section 6. Conclusions are outlined in Section 7.

2 Modeling and Identification

The most basic reflex arc is comprised of a motoneuron, a skeletal muscle fiber, and a DRG neuron. From a simple systems perspective, the reflex arc is a length/velocity feedback control loop. Motivated by anatomy, mathematical viability, and the state-of-the-art in biomodeling techniques, this control loop is segmented into simple input-output blocks. While anatomical partitions permit one to individually examine and construct experimental *in-vitro* testbeds with an aim to identify models for these components of the reflex arc, mathematical partitions (wherever possible) facilitate analytical procedures and testing of anatomical components with complex nonlinearities that may be difficult to identify in a single stage. Existing literature provides for simple input-output models for these sub-components. Despite the extensive amount of experimental data and mathematical models available in literature, the authors were able to identify an area where there is ample scope for improvement. Literature survey suggests that there are not many results presented that simulate the complete closed-loop response of the stretch reflex arc and its modulation by descending signals. In order to develop quantitative models for brain activity, simple controllers can be designed to: i) regulate this closed-loop response to a desired equilibrium, and ii) allow the muscle length to track a desired trajectory that is completely specified in time. In the following paragraphs, the presentation provides the initial models that are utilized in an integrated simulation study.

2.1 Motoneuron Model

In this study, it is assumed that the inputs to the motoneurons (See (a) in Figure 1) are descending supraspinal command signals (See (k) in Figure 1) as well as a length/velocity feedback signal (See (j) in Figure 1) through the DRG neurons. The motoneuron is typically modeled as a bandpass filter [19, 20, 21] spanning a range of motoneuron firing rates [4]

$$\frac{m(s)}{i(s)} = \frac{\left(\frac{s}{33}\right)^2 + \left(\frac{s}{33}\right) + 1}{\left(\frac{s}{58}\right)^2 + 2\left(\frac{s}{58}\right) + 1} \tag{1}$$

where $m(s)$ denotes the number of pulses per unit time [ps^{-1}] output by the motoneuron while $i(s)$ denotes the combined pre-synaptic current input measured in [nA]. The firing rate of the motoneurons determines the amount of active force that the contractile element in the muscle is able to generate; hence, the true output of the motoneuron is the number of pulses obtained in a unit of time at the nerve-muscle junction. Since the post-synaptic action potential generated in a motoneuron must travel the length of the neuronal axon into the body of the muscle fiber, the phase lag introduced by this simple pulse conduction must also be taken into consideration in any reasonable model of the reflex arc.

2.2 Isometric Force Generation Dynamics

The input to this component is the output of the motoneuron, namely an action potential train arriving at the neuromuscular junction (this junction exhibits a chemical synaptic

interface). The released AcH leads to the release of Ca++ inside the extrafusal muscle fiber. This component is modeled by a linear low-pass filter response [22]

$$\dot{q}(t) = -\alpha q(t) + w(t) \tag{2}$$

where $w(t) \in \Re^1$ represents an input impulse train, $q(t)$ is considered to represent the $Ca{+}{+}$ concentration in the muscle, and α is a muscle-specific constant that represents the pole of this first-order filter. Since the $Ca{+}{+}$ concentration cannot increase indefinitely, a static saturation nonlinearity is introduced to limit the effect of the released $Ca{+}{+}$ [22]

$$\gamma = \frac{q^2}{q^2 + k^2} \tag{3}$$

where $\gamma(t) \in \Re^1$ represents the useful amount of $Ca{+}{+}$ concentration, $q(t)$ has been previously defined in (2) and k is a muscle specific constant. This release of the neurotransmitter leads to molecular activity which underlies the conversion of chemical energy into work energy. This phenomenon is modeled by a nonlinear low-pass filter [22]

$$\dot{a} = b_0(1 - b_1 a)^2(\gamma - a) \quad 0 \leq b_1 \leq 1 \tag{4}$$

where $b_0, b_1 \in \Re^1$ are muscle-specific constants. Thus, the muscle activation dynamics can be represented by a cascade of a linear and a non-linear low pass filter interjected by a static nonlinearity (See (f) in Figure 1). The output of this cascade, denoted by $a(t)$, is a normalized hypothetical isometric force that the muscle fiber generates in response to motoneuron stimulation.

2.3 Passive and Active Force Models

The force developed in skeletal muscle fibers consists of two parts: i) the passive elastic stiffness force (See (b) in Figure 1) of the muscle, and ii) the active force (See (e) in Figure 1) generated by the contractile element. Both the passive and active forces, denoted by $F_p(x(t), \dot{x}(t))$ and $F_a(x(t), \dot{x}(t))$, respectively, are nonlinearly dependent on the length and the velocity of the fiber as follows [4]

$$\begin{array}{c} F_p = f_p(x) + B_p \dot{x} \\ F_a = a F_{\max} f_x f_v \end{array} \tag{5}$$

where $x(t), \dot{x}(t)$ denote, respectively, the length and velocity of the muscle fiber, $a(t)$ has been previously defined in (4), $F_{\max}$ is defined as the peak isometric force produced by the muscle, while specific implementations for the nonlinearities $f_p(x(t))$, $B_p(x(t))$, $f_x(x(t))$, and $f_v(\dot{x}(t))$ can be obtained as in [4].

2.4 Encoding Model

The continuous time stretch of the spindle is translated to a spike train in the afferents. This phenomenon is often studied via a process that is referred to as encoding (See (h) in Figure 1). A neuron can be seen as mapping a continuous time signal to an impulse

train with the firing frequency encoding the amplitude of the signal. In order to convert the continuous spindle output to a spike train, the idea of an encoder is utilized. However, since a neuron is only able to encode positive signals above a specified threshold, the idea of on/off cells has been effectively utilized in literature [8]. The encoding of the continuous spindle stretch output signal into a pulse train can be represented by a nonlinear ordinary differential equation which is easily obtainable from the model of Hodgkin and Huxley [23]. For the purpose of this paper, we utilize the following simplified equation [24]

$$\begin{array}{c} C\dot{v}_m = -m_\infty\left(v_m - e_{Na}\right) - 26r\left(v_m - e_K\right) + i_{in} \\ \dot{r} = \dfrac{r_\infty - r}{\tau_r} \end{array} \tag{6}$$

where $v_m(t)$ denotes the membrane potential, $i_{in}(t)$ denotes the input stimulus, e_{Na}, e_K represent the constant equilibrium potentials of the Na and K channels, respectively, τ_r denotes a time constant that determines the width of a spike, while $m_\infty\left(v_m(t)\right)$ and $r_\infty\left(v_m(t)\right)$ denote second order polynomials

$$\begin{array}{l} m_\infty = 17.8 + 47.6v_m + 33.8v_m^2 \\ r_\infty = 1.24 + 3.74v_m + 3.2v_m^2 \end{array} . \tag{7}$$

2.5 Muscle Spindle Model

The muscle spindle (See (d) in Figure 1) is the primary sensory component in the reflex arc that is connected in parallel with the extrafusal muscle fibers. From a systems perspective, the spindle is a sensor with nonlinear dynamics. The stretch seen by the sensory region in the spindle is proportional to the tension as a first order approximation. The mechanical filtering process that converts the change in muscle length to the extension of the spindle can be represented by the following nonlinear ordinary differential equation [4, 25]

$$\dot{z} = \dot{x} - f_i\left(\frac{bz}{f_l(x - z - c)}\right) \tag{8}$$

where $z(t)$ represents the length of the spindle sensory region, $x(t)$ denotes the length of the muscle, c is a constant that denotes the slack length of the spindle, while $f_l\left(x(t)\right)$ denotes a nonlinear stiffness for the spindle contractile region that is defined as follows [4]

$$f_l(x) = \begin{cases} 0.0009197\exp(400x) & x < 0.0025 \\ x & x \geq 0.0025 \end{cases} \tag{9}$$

while $f_i\left(\lambda(t)\right)$ denotes a force-velocity function for lengthening and shortening of the spindle [4]

$$f_i(\lambda) = \begin{cases} \dfrac{1-\lambda}{c_2\lambda - c_1} & \lambda \geq 1 \\ \dfrac{\lambda - 1}{c_3 + c_4\lambda} & \lambda < 1 \end{cases} . \tag{10}$$

where $c_1 = 0.0855$ sm^{-1}, $c_2 = 0.0227$ sm^{-1}, $c_3 = 0.001$ sm^{-1}, $c_4 = 0.0628$ sm^{-1}. In this simplified study, we do not account for spindle conditioning via $\gamma-$motoneurons. However, $f_l\left(x(t)\right)$ defined in (9) above prevents a model discontinuity if the spindle goes slack.

It is well known that the *Ia* afferents are sensitive to both the length $z(t)$ and velocity $\dot{z}(t)$ of spindle stretching while the Group *II* afferents are sensitive only to the length $z(t)$ of the spindle. Thus, the receptor potential $r(t)$ (See (j) in Figure 1) collectively induced in the afferents can be modeled linearly as follows [25]

$$r = K_p z + K_v \dot{z} \tag{11}$$

where K_p and K_v are constants. From a systems perspective, this is akin to defining a filter tracking error variable or a sliding surface [26].

2.6 DRG Neuron Model

For purposes of this study, the DRG neuron can be modeled as a unity transfer function element. To make the model more realistic, the neuron can also be modeled as a pure delay element. Since the DRG neuron makes a monosynaptic electrical synapse with the motoneuron, the dynamics for the DRG neuron can be lumped with the acquired transfer function for the motoneuron. Experimentally, this implies that the axon of the DRG neuron would be electrically stimulated with appropriate excitation signals while the spike train recorded at the motoneuron-muscle junction would be treated as the output.

3 Problem Formulation

An integrated simulation model is developed to analyze the transient as well as steady state response of a single motor unit under the effect of step disturbances of varying magnitudes. The open-loop muscle dynamics evolve via the following Newtonian equation for motion

$$M_m \ddot{x} + F_p(x, \dot{x}) + aF_{\max} f_x(x) f_v(\dot{x}) = F_L \tag{12}$$

where $x(t), \dot{x}(t), \ddot{x}(t) \in \Re^1$ represent the length, velocity and acceleration of the muscle, respectively, M_m represents the mass of the muscle, $F_p(x(t), \dot{x}(t))$ is the passive force generated by the muscle fiber as defined in (5), $a(t)$ denotes the control input, $f_x(x(t)), f_v(\dot{x}(t))$ represent muscle force modulations with change in length and velocity, while $F_L(t) \in \Re^1$ denotes the disturbance force that acts on the muscle fiber to perturb it from its equilibrium resting position. As the muscle stretches or contracts as dictated by the dynamics of (12), the muscle spindle (that sits in parallel with the muscle) exhibits a dynamic response previously defined in equations (8-10). This generates a strain in the afferent fibers wrapped around the sensory region of the spindle which is encoded into a series of spikes (See equations (6-7)) which eventually synapse with motoneurons in the spinal cord. Also impinging on the motoneuron are the axons of neurons from supraspinal regions that encode the activity of the brain. The bandpass response of the motoneuron has been modeled as in (1). The combined motoneuron input current then travels down to the nerve-muscle junction where the dynamics of (2-4) actively generate force in the muscle (through the input $a(t)$) in order to bring it to another equilibrium length. Mathematically, the control problem can be represented by defining an error variable $e(t) \in \Re^1$ as follows

$$e = x - x_{eq} \tag{13}$$

where x_{eq} can be obtained as a solution of the algebraic equation (with a constant disturbance F_L and pure reflex action)

$$F_p\left(x_{eq},0\right)+a\left(x_{eq}\right)F_{\max}f_x\left(x_{eq}\right)=F_L. \tag{14}$$

The closed-loop of the reflex arc then tries to nullify the signal $e\left(t\right)$.

Remark 1 *In the presence of a constant supraspinal command u, an equilibrium muscle length can be obtained by solving the following algebraic equation*

$$F_p\left(x_{eq},0\right)+a\left(x_{eq},u\right)F_{\max}f_x\left(x_{eq}\right)=F_L \tag{15}$$

where $a\left(x_{eq},u\right)$ denotes the normalized active isometric force produced in response to the supraspinal input $u\left(t\right)$ at muscle length x_{eq}.

4 Simulation Results

Utilizing the muscle dynamic model of (12) as well as the dynamics of the plant modeled by (1-11), simulation studies were conducted in SIMULINK. A block diagram of the model can be seen in Figure 1. To resolve compatibility issues between the various blocks, the neuronal pulses have been distinguished from digital pulses. The model for the isometric force generation dynamics given by equations (2-4) requires digital pulses which are then integrated (roughly) to produce a continuous output signal. However, the encoder dynamics of (6) generate outputs which correspond to neuronal pulses. To ensure coherence, a relay element is utilized to convert neuronal pulses to digital pulses.

The first simulation study was conducted to obtain the transient response of the muscle under a step disturbance. Pure reflex action as well as the effects of descending inputs was analyzed. The initial conditions for the muscle state variables were selected as follows

$$x=36\text{ mm}\quad \dot{x}=0\text{ mms}^{-1} \tag{16}$$

The optimum muscle fiber length was somewhat arbitrarily chosen to be $x_{opt}=40$ [mm]. Since the applied disturbance is expected to obtain a larger equilibrium length, the choice of $x_{opt}=40$ [mm] ensures that we would be operating around the region where the active force generation F_a is maximal. The peak isometric force that the muscle is able to generate was fixed at $F_{\max}=100$ [N]. A nominal load of 8.82 [N] was applied to the muscle fiber and its transient response was obtained. Next, a series of brain/supraspinal commands $u_i\left(t\right)$ (with $u_{i+1}>u_i$) were applied to the motor unit. Supraspinal commands were simulated via additive presynaptic inputs to the motoneuron as can be seen in Figure 1. The transient performance of the muscle fiber length under incremental brain commands are shown in Figure 2. The arrow denotes direction of increasing supraspinal activity. The transient response is seen to be identical for all the curves since it is governed mainly by the ratios K_p/M_m and K_v/M_m. We note that this neglects the minimal influence of the muscle passive forces which are about 5% of active muscle forces. The steady-state (equilibrium) values for muscle length are different as expected since they are approximately governed by the ratio $\left(F_L-f\left(u,\bar{x}\right)\right)/K_p$ where $a\left(u\right)$ is a positive function that denotes the active muscle force

produced in response to a pre-synaptic motoneuron input $u(t)$ when the muscle is stationary with length $\bar{x}$. From a simple systems perspective, a constant disturbance matched with the input would produce a steady-state error for this system with no integrators in the loop. From a anatomical perspective, the same amount of disturbance can obtain a continuum of equilibrium points for the muscle length – these equilibria are modulated by the amount of descending control.

The second simulation study was conducted in order to study the response of the muscle to a time-varying disturbance modeled as

$$F_L(t) = 8.82 + 4.9\sin(2\pi t) \text{ [N]}. \tag{17}$$

The muscle was first allowed to settle down to an equilibrium length ($x = 37$ [mm]) for a disturbance load $F_L(t^-) = 8.82$ [N]. No additive supraspinal command was issued. At time $t = 0$, the sinusoidal disturbance input was applied. The muscle length then shows an approximate sinusoidal response as can be seen in Figure 3 (In the interest of clearer representation amenable to meaningful analysis, both the muscle length and the load force have been shown to vary around 0 and then have been normalized to lie between -1 and 1. The data along the ordinate is thus dimensionless). It is noticed that the muscle length changes more in the negative direction than in the positive direction. This is attributable to the fact that the muscle gets closer to our arbitrarily chosen optimal length of 40 [mm] when moving positive while it gets further away from its optimal length when moving negative. Thus, for a given change in absolute length, it can generate more force in the positive direction than it does in the negative direction. It can also be noticed that the muscle response is smoother in the positive direction than it is in the negative direction. This is due to the fact that the muscle is approaching tetanus as its absolute length increases. In the other direction, the muscle shows a twitchy transient response which is a consequence of the larger interspike interval in the post-synaptic pulse train. The phase lag shown in 3 is a consequence of the sinusoidal disurbance filtering through a second order system.

The third simulation study was conducted to study the steady-state response of the muscle under step disturbance and from thereon to deduce the relationship between the applied disturbance and the equilibrium length of the muscle. For a single run of the simulation, the amount of supraspinal input $u_i(t)$ was fixed, while the applied load F_L was incremented in steps of $0.2g$ [N]. The steps were spaced so as to allow enough time for the muscle fiber to obtain an equilibrium position. The load was varied between a minimum of $0.5g$ [N] and a maximum of $2.5g$ [N]. The set of equilibria thus obtained was plotted against the total force $(F_p + F_a)$ generated by the muscle. The data obtained was then fit on a second order polynomial curve in the least squares sense. Since the data obtained was for suboptimal lengths tending to the optimal length of the muscle (as disturbance is incremented), the curve obtained was not linear but the ratio $\dfrac{\triangle F}{\triangle x_{eq}}$ tended to increase as $x_{eq} \to x_{opt}$. This can be explained on the basis of experimental studies as well as the choice of $f_x(x)$ as given in [4]. The data obtained can be seen in Figure 4. The direction of the arrow indicates increasing supraspinal activity $u_i(t)$. As is obvious from Figure 4, different amounts of brain activity generate different length equilibria for the muscle, this study can be used as a stepping stone to obtaining a quantitative analysis of the behavior and impact of supraspinal commands that modulate the stretch reflex arc and allow for a variety of voluntary movements. It can

be noticed from the data obtained that (at least, in the region of interest) $\frac{\triangle x_{eq}}{\triangle u}$ is seen to be independent of the disturbance force F_L.

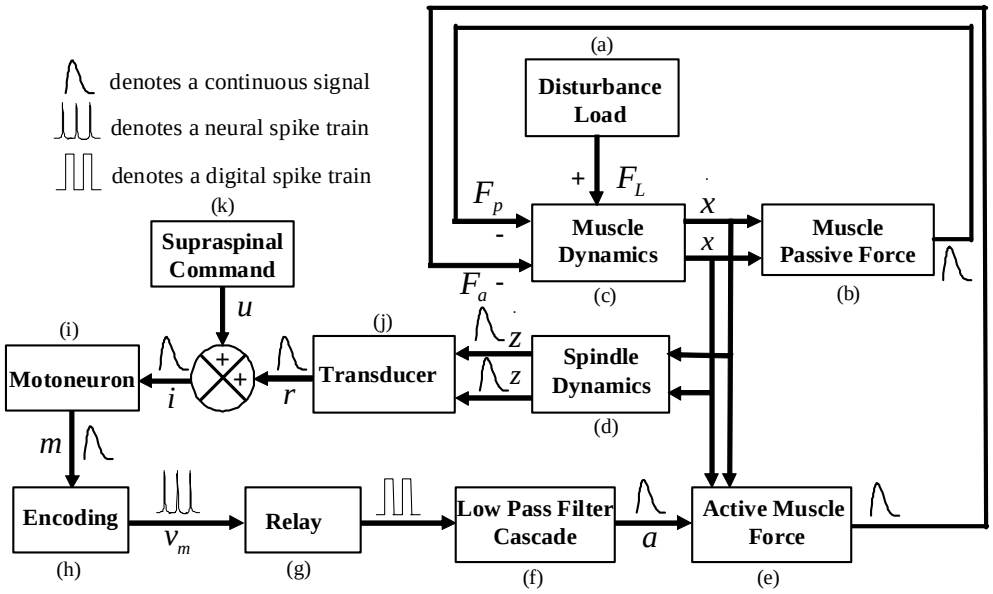

Figure 1: Block Diagram of Simulink Model

5 Future Systems Work

Having obtained an estimate for the supraspinal command about the nominal operating point of the muscle, we are now in a position to develop control inputs $u(t)$ that achieve a desired equilibrium muscle length or the tracking of an arbitrary desired trajectory in time. (Although we use the terminology $u(t)$ in the interest of here, $u(z(t), \dot{z}(t))$ is a better notation, because the cerebral cortex utilizes the *Ia* and *II* afferent input that reaches the brain along ascending pathways to output a descending supraspinal command). Given the dynamic models of biological components that comprise the reflex arc, the development of control strategies can now be initiated such that they give an adequate response not only around the muscle optimal length but also over a wide set of lengths where the muscle can be expected to work at within the constraints imposed by joint limits. Over the last 15 years, extensive work has been done in the design and the experimental validation of advanced model-based controllers for mechatronic systems (*e.g.*, [27, 28]). The control design philosophy is based on the belief that enhanced closed-loop performance can be achieved by designing model-based controllers as opposed to controllers based on simplified, reduced, and/or linearized models. Due to the inherent difficulties associated with the dynamic structure of nonlinear systems, previous control design methods often utilized simplifying assumptions to aid the control synthesis; however, recent Lyapunov-based control design techniques have formed a theoretical basis for the design of high-performance control strategies. The future

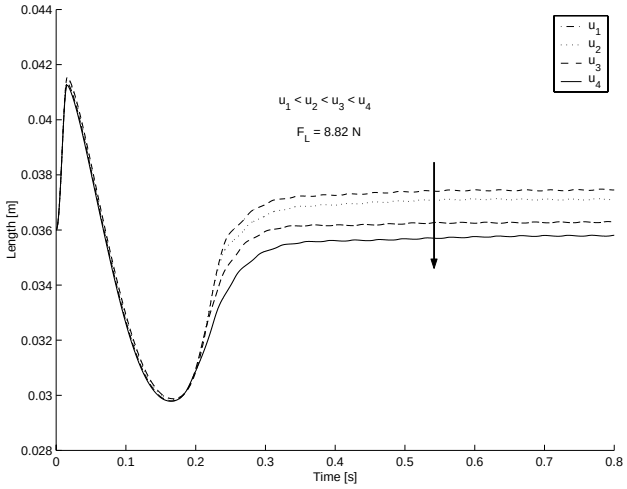

Figure 2: Step Response of Muscle Fiber

aspect of our research will involve setting up the regulation/tracking control problem for the muscle and then the design/analysis of Lyapunov-based controllers that will mimic quantitatively and analytically the supraspinal modulation of the reflex arc. This is in contrast with schemes that are based on neural networks that tend to bloat up computationally as well as get training-intensive once the complexity of the desired functionality is increased.

6 Experimental Testbeds and Preliminary Data

As stated previously, current literature only relies on *in-vivo* testing and identification procedures where expansive and exhaustive isolation of components is not possible. Additionally, *in-vivo* construction of the components of the reflex arc may not mimic their *in-vitro* counterparts and thus may not conform to existing modeling data; however, these *in-vivo* models do provide a starting point for the synthesis of the *in-vitro* counterpart. Hence, it is our belief that properly designed experimental *in-vitro* testbeds will give one the ability to examine all components of the reflex arc including input-output relationships for the motoneuron, the DRG neuron, as well as the stretch dynamics for the extrafusal and intrafusal muscle fibers. In what follows, we will describe the experimental testbeds that will be setup to identify the *in-vitro* sub-components that are being fabricated in the Nanoscience Center at University of Central Florida (UCF). Some preliminary experimental data is also provided.

Motoneurons: Motoneurons from the spinal cords of rat embryos (E-14) have been isolated in the Nanoscience Center at UCF and the culture conditions for long-term survivability have been standardized [14]. In Figure 5, we show rat embryonic motoneurons that were cultured on glass coverslips coated with a self-assembled monolayer (N-1[3-(trimethoxysilyl) propyl] diethylenetriamine; DETA) in serum-free medium according to published protocols [14]. On day 9 of the culture, conventional whole-cell patch clamp measurements (Figure 5a) were performed and the repetitive firing properties of the motoneurons were measured in current clamp mode with 1 [s] current injections (Figure 5b.) For the standardization of the data, the injected current (input) was multiplied with the membrane resistance of the

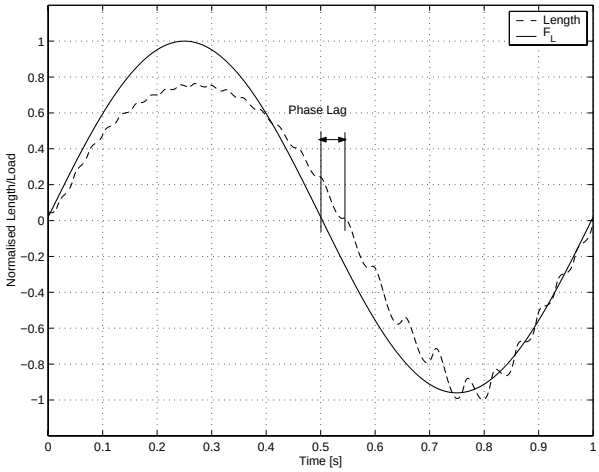

Figure 3: Transient Response of Muscle to Sinusoidal Disturbance

cell. (Repetitive firing is evoked by membrane depolarizations. The depolarization of the membrane is linearly related to the injected current and the membrane resistance). The number of evoked action potentials were counted during the 1 [s] stimulation period. Data were expressed as mean ±SEM (n=8) (See Figure 5c).

The linear relationship expressed in (1) is generated from experimental data obtained by using sinusoidal pre-synaptic input currents. Since a motoneuron input/output map is known to be highly nonlinear, sinusodial transfer functions reveal no information about the response to arbitraty inputs. At the present time, we are conducting preliminary studies for identification of the cultured motoneurons by the use of orthogonal Wiener kernel formulation employing the Lee-Schetzen technique of cross correlation [29]. This method provides with a mathematical description of the physiological system that can then be employed to theoretically predict the output of the equivalent physiological system for an arbitrary input. A single electrode patch clamp would be utilized for stimulation and measurement purposes.

Isometric Muscle Force Dynamics: Since polarized growth of motoneurons and muscle fibers on micro-cantilevers have already been demonstrated in the Nanoscience Center at UCF (in the same environment as we described for motoneurons), we are poised to setup experiments for identification of muscle force dynamics using electrophysiology or/and confocal microscopy. An experimental testbed would be created to determine the parameters that govern the response of the quasi-linear models of (2-4). In order to study the input-output characteristics, a polarized motoneuron innervating an extrafusal muscle fiber would be identified in culture. Under isometric conditions, a transducer would measure generated active muscle force in response to a spike train at the neuromuscular junction – the output of the transducer would be proportional to the output signal $a\,(t)$ of (4) above. With the appropriate muscle fiber displacement and force measurements, a study of the input-output data obtained from electrical stimulation of the motoneuron would facilitate identification of the parameters that govern the response of the filters. A good fit between theory and experiment would authenticate the model; a poor fit would indicate presence of nonlinearities, and hence, further addition of nonlinear terms and re-tuning of the parameters would

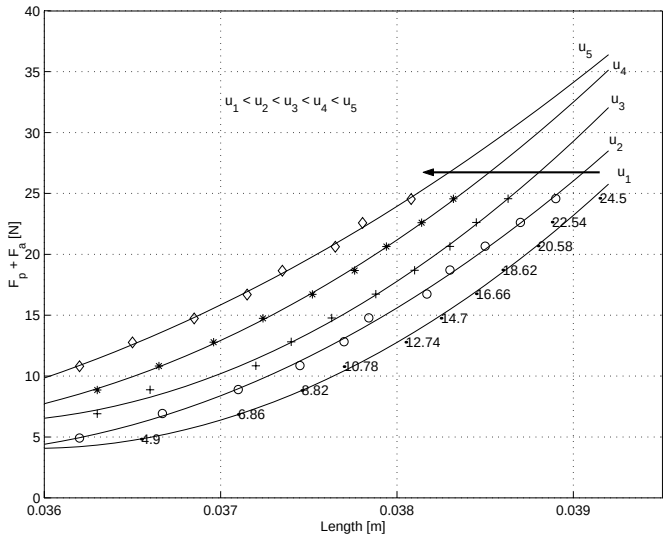

Figure 4: Muscle Force vs Muscle Equilibrium

be required.

Muscle Active and Passive Force Generation: In order to validate the passive force generation model, one requires the ability to apply variable load forces on the muscle and the ability to continuously monitor the length of the muscle. After severing the motoneuron-muscle synapse, the muscle would be passively stretched to validate the expression for passive force generation in the muscle as a function of length and velocity in the following manner. First, the nonlinear length function $f_p\left(x\left(t\right)\right)$ would be determined at muscle equilibrium position when there is no dependence on velocity and then the dynamic data and the acquired length function would be utilized to determine the remainder of the nonlinearity (*i.e.,* $B_p\left(x\left(t\right)\right)$). In order to determine the active force generation model, a testbed would be constructed with the twin abilities to electrically stimulate the motoneuron and continuously monitor the length of the muscle fiber. After severing the DRG-motoneuron synapses, the muscle fiber would be stimulated through the motoneurons in an open-loop fashion to validate the model as follows: i) determine the nonlinear length function $f_x\left(x\left(t\right)\right)$ at muscle equilibrium position when there is no dependence on velocity, and ii) utilize the dynamic data and the acquired length function to determine the velocity dependence $f_v\left(\dot{x}\left(t\right)\right)$.

Encoding Model: In order to validate our choice of parameters, we require a testbed with the abilities to innervate cultured intrafusal muscle fibers with afferents and the achievement of a desired stretch profile for the spindle. After isolating the spindle and the afferents, the spindle would be tensioned at different frequencies and the discharge in *Ia* afferents recorded to establish the relationship between spindle output and afferent discharge.

Spindle Model: In order to validate the dynamics of the spindle, one needs to be able to stimulate the motoneuron with a class of test inputs and monitor the spike train obtained in the afferents emanating from the spindle. After severing the DRG-motoneuron synapses, the nonlinear spindle dynamics would be identified as follows: i) electrically stimulate the motoneuron with a class of inputs and record the spike train obtained in the afferents, ii) utilize the input-output motoneuron observations and a prior knowledge of the encoding

transfer function to identify the nonlinearities in the dynamics, and iii) tune model parameters and add nonlinear terms to the model to obtain a good fit between recorded data and the mathematical model.

7 Conclusions

In this paper, we have presented simulation results for the closed-loop response of the stretch reflex arc. The simulation results show that the integrated model is able to mimic the qualitative response of the stretch arc obtained though *in-vivo* studies that have been reported extensively in literature. At the system levels, our future work would involve drawing a map between supraspinal activity and muscle movement. We also reported preliminary data concerning an experimental identification and implementation of the stretch reflex arc *in-vitro*. Our future work will involve isolating the remaining components of the reflex arc in culture and then the ability to successfully integrate selected components as described in the section on experimental testbeds. This will enable us to gather pertinent input-output data for successful system identification.

References

[1] C.C.A.M. Gielen and J. C. Houk, "A Model of the motor servo: Incorporating non1inear spindle receptor and muscle mechanical properties", *Bio. Cybern.,* 57, pp. 217-231, 1987.

[2] M. Hollerbach and C.G. Atkeson, "Deducing planning variab1es from experimental arm trajectories: Pitfalls and possibilities", *Bio. Cybern.,* 56, pp. 279-292, 1987.

[3] C.C.A.M. Gielen, J.C. Houk, S.L. Marcus, and L.E. Miller, "Viscoelastic properties of the wrist motor servo in man", *Am. Biomed. Eng.,* 12, pp. 599-620, 1984.

[4] J. He, M.G. Maltenfort, Q. Wang, and T.M. Hamm, "Modeling Neural Control", *IEEE Control Systems Magazine*, 21,(4), pp. 55-69, August 2001.

[5] A.V. Hill, "The heat of shortening and dynamic constants of muscle", *Proc. Royal Society of London*, B126, pp. 136-195, 1938.

[6] J. M. Winters and L. Stark, "Muscle Models: What is gained and what is lost by varying model complexity", *Biol. Cybern.*, 55, pp. 403-420, 1987.

[7] C. Wu, J. C. Houk, K.Y. Young, and L.E. Miller, *Nonlinear Damping of Limb Motion*, in J.M. Winters and SL-Y Woo (Eds) Multiple Muscle Systems, Springer Verlag, pp. 214-235, 1990.

[8] B.K. Ghosh and Z. Nenadic, "Signal Processing and Control Problems in the Brain", *IEEE Control Systems Magazine*, 21 (4), pp. 28-41, August 2001.

[9] R.E. Allen, et al., "A Serum-Free Medium That Supports the Growth of Cultured Skeletal-Muscle Satellite Cells", In Vitro Cellular & Developmental Biology, 21 (11), pp. 636-640, 1985.

[10] J.C. Martinou, et al., "Characterization of two factors enhancing choline acetyltransferase activity in cultures of purified rat motoneurons", *Journal of Neuroscience,* 9 (10), pp. 3645-3656, 1989.

[11] A.E. Schaffner, P.A. St John, and J.L. Barker, "Fluorescence-activated cell sorting of embryonic mouse and rat motoneurons and their long-term survival in vitro", *Journal of Neuroscience*, 7 (10), pp. 3088-3104, 1987.

[12] R.I. Schnaar and A.E. Schaffner, "Separation of cell types from embryonic chicken and rat spinal cord: characterization of motoneuron-enriched fractions", *Journal of Neuroscience*, 1 (2), pp. 204-217, 1981.

[13] M.J. Strong and R.M. Garruto, "Isolation of fetal mouse motor neurons on discontinuous Percoll density gradients", *In Vitro Cell Developmental Biology*, 25 (10), pp. 939-945, 1989.

[14] M. Das, P. Molnar, et al., "Characterization of rat embryonic motoneurons in a defined system", Progress in Biotechnology, vol. 19, pp. 1756-1761, 2003.

[15] M. Feemster, D. Dawson, A. Behal, and W. Dixon, "Tracking Control in the Presence of Nonlinear Dynamic Frictional Effects: Robot Extension", *Asian Journal of Control*, 1 (3), pp. 153-168, 1999.

[16] M. Feemster, P. Vedagarbha, D.M. Dawson, and D. Haste, "Adaptive Control Techniques for Friction Compensation", *Mechatronics - An International Journal*, 9, pp. 125-145, 1999.

[17] A. Behal, M. Feemster, D. M. Dawson, and A. Mangal, "Partial State Feedback Control of Induction Motors with Magnetic Saturation: Elimination of Flux Measurements", *Automatica,* 38 (2), February 2002.

[18] M. Feemster, A. Behal, P. Aquino, and D.M. Dawson, "Tracking Control of the Induction Motor in the Presence of Magnetic Saturation Effects", *Proc. of the IEEE Conference on Decision and Control*, Phoenix, AZ, pp. 341-346, December 1999.

[19] F. Baldissera, P. Campadelli, and L. Piccinelli, "The dynamic response of cat a motoneurons investigated by intracellular injection of sinusoidal currents", *Exp. Brain*, 1984.

[20] C. Christakos, "The mathematical basis of population rythms in nervous and nervomuscular systems," *Int. J. Neurosci.*, 29, pp. 103-107, 1986.

[21] P. Matthews, "Spindle and motoneuronal contributions to the phase advance of the human stretch reflex and the reduction of tremor", *J. Physiol.*, 498, pp. 249-275, 1997.

[22] J. Bobet and R. Stein, "A simple model of force generation by skeletal muscle during dynamic isometric contractions", *IEEE Trans. Biomed. Eng.*, 45, pp. 1010-1016, 1998.

[23] A.L. Hodgkin and A.F. Huxley, "A quantitative description of membrane current and its application to conduction and excitation in nerve", *Journal of Physiology,* 117, pp. 500-544, 1952.

[24] H.R. Wilson, "Simplified Dynamics of human and mammalian neurocortical neurons", *Journal of Theoretical Biology*, 200, pp. 375-388, 1999.

[25] Z. Hasan, "A mode1 of spindle afferent response to muscle stretch", *J. Neurophysiology*, 49, pp. 989-1006, 1983.

[26] F.L. Lewis, C.T. Abdallah, and D. M. Dawson, *Control of Robot Manipulators*, Macmillan Publishing Co., NY, 1993.

[27] D.M. Dawson, J. Hu, and T.C. Burg, *Nonlinear Control of Electric Machinery*, Marcel Dekker, ISBN 0-8247-0180-1, 1998.

[28] M. S. de Queiroz, D.M. Dawson, S. P. Nagarkatti, and F. Zhang, *Lyapunov-Based Control of Mechanical Systems*, Birkhauser, ISBN 0-8176-4086-X, 1999.

[29] Marmarelis and Marmarelis, *Analysis of physiological systems*, Plenum Press, New York, 1978.

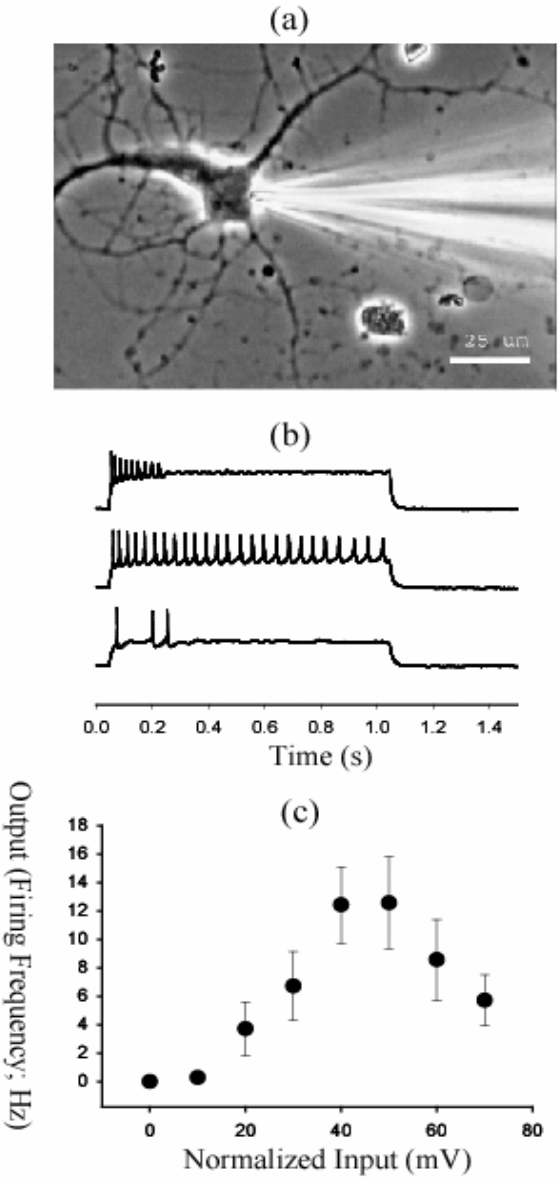

Figure 5: Measurement of Static Input /Output Function of Motoneurons Cultured in a Defined Environment